

Averaged Switch Modeling of Boundary Conduction Mode Dc-to-Dc Converters

Jingquan Chen, Robert Erickson, and Dragan Maksimović

Colorado Power Electronics Center
Department of Electrical and Computer Engineering
University of Colorado at Boulder
Boulder, CO 80309-0425, USA

Abstract – Averaged switch approach is extended to the modeling of boundary conduction mode (BCM) dc-to-dc converters that operate at the boundary between continuous conduction mode (CCM) and discontinuous conduction mode (DCM). BCM dc-to-dc converters have smaller inductor size and reduced switching losses compared to CCM, and lower peak current compared to DCM. The large-signal BCM averaged switch model shows that several BCM converters with input voltage feedforward exhibit resistive or nearly resistive input characteristic, which is well suited for realization of power factor correctors. It is shown that BCM converters exhibit simpler dynamics compared to CCM current programmed control (CPM). Small-signal frequency responses predicted by the averaged switch model are verified by simulation and experiments.

I. INTRODUCTION

Pulse-width modulation (PWM) at constant switching frequency is a common technique applied in electrical power conversion circuits. Switching converters are usually operated in continuous conduction mode (CCM) for higher power applications or at full load, and in discontinuous conduction mode (DCM) for lower power application or at light load. Averaged models for constant-frequency CCM or DCM converters are well known and accepted in practice.

Converters controlled to operate at the CCM/DCM boundary are said to operate in boundary conduction mode (BCM) or critical conduction mode. As an example, circuit diagram of a BCM boost converter is shown in Fig. 1. A switching cycle is initiated by turning the transistor on when the diode current drops to zero, while the turn-off transition is triggered when the peak transistor current reaches a desired value. The diode recovery problem is removed because the diode current is zero at the time when the transistor turned on. In contrast to constant-frequency PWM, the switching frequency of BCM converter varies with changes in the load current or the input voltage. BCM is frequently used in low-power power-factor-correction (PFC) rectifier applications [1-4].

In this paper, the averaged switch modeling approach is extended to modeling of BCM converters. The averaged switch modeling is briefly reviewed in Section II. In Section III, we consider BCM converters without input voltage feedforward. Large-signal averaged models are derived for basic converter configurations. Parameters of linearized, small-signal averaged switch models are derived and used to

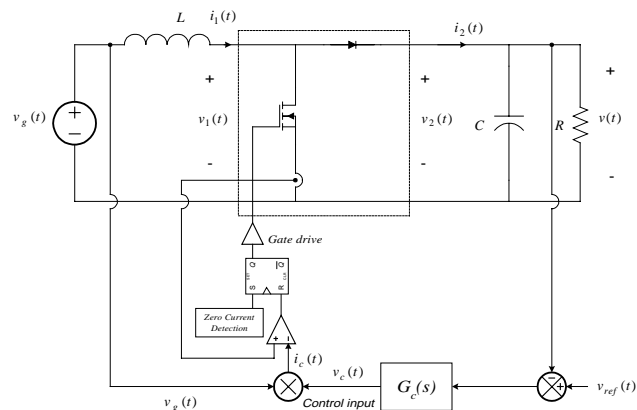


Fig. 1 Boundary conduction mode incorporating input voltage feedforward.

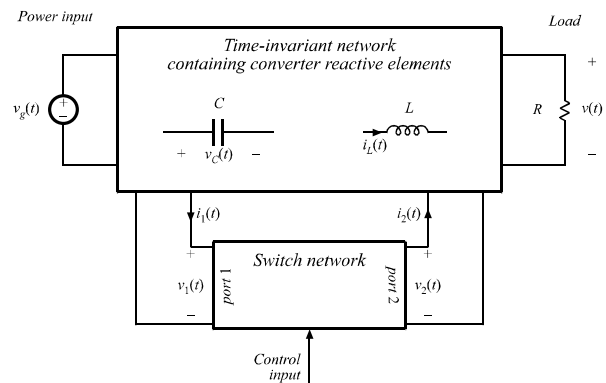


Fig. 2 Averaged switch modeling: a switch network, containing only the converter switching elements.

obtain expressions for salient features of frequency responses of BCM converters. Modeling of BCM converters with input voltage feedforward is described in Section IV. The averaged models lead to simple explanation of how BCM converters can be well suited for PFC applications. In Section V, computer simulations and experimental results are used to illustrate applications and validate the BCM averaged switch models.

II. AVERAGED SWITCH MODELING

Averaging has been well accepted as an effective way to model low-frequency components of waveforms in PWM switching converters [1, 6-10]. The switching frequency and the harmonics are removed by averaging the waveforms over a switching cycle. To arrive at an averaged circuit model, it has been recognized that only the waveforms of the switching elements need to be averaged, leading to averaged switch modeling approach [1, 10-14]. Fig. 2 illustrates how to distinguish a switch network in a switching converter. The terminal waveforms of the switch network are then averaged over a switching cycle. Based on the averaged terminal quantities, the switch network is then replaced by basic circuit elements, such as dc transformer, dependent or independent voltage or current source, loss-free resistor, power source, or power sink [1, 14-17]. The resulting large-signal equivalent circuit is suitable for circuit-oriented computer simulation. Small-signal models can be obtained by linearization of the large-signal averaged equivalent circuit.

III. BOUNDARY CONDUCTION MODE WITHOUT INPUT VOLTAGE FEEDFORWARD

A. Averaged switch model

Let's consider the boost converter of Fig. 3(a) as an example. The switch network and terminal voltage and current waveforms are illustrated in Fig. 4 for BCM operation. While the transistor conducts in the first subinterval, the inductor current increases from zero at a slope of v_g/L until it reaches the peak current equal to the control input i_c . At this time, the transistor is turned off and the diode starts to conduct. The inductor current begins to drop with a slope of $(v_g-v)/L$ until it reaches zero at the end of the second subinterval. At this time, the transistor is turned on again.

The averaged switch network quantities in (1) to (4) are found by averaging the respective waveforms of Fig. 4 over one switching period:

$$\langle i_1(t) \rangle = \frac{\langle i_c(t) \rangle}{2} \quad (1)$$

$$\langle i_2(t) \rangle = \frac{t_{off}}{t_s} \frac{\langle i_c(t) \rangle}{2} \quad (2)$$

$$\langle v_1(t) \rangle = \frac{t_{off}}{t_s} \langle v(t) \rangle \quad (3)$$

$$\langle v_2(t) \rangle = \langle v(t) \rangle \quad (4)$$

Equation (1) implies that the input current is controlled to be one half of the peak inductor current, which is equal to the

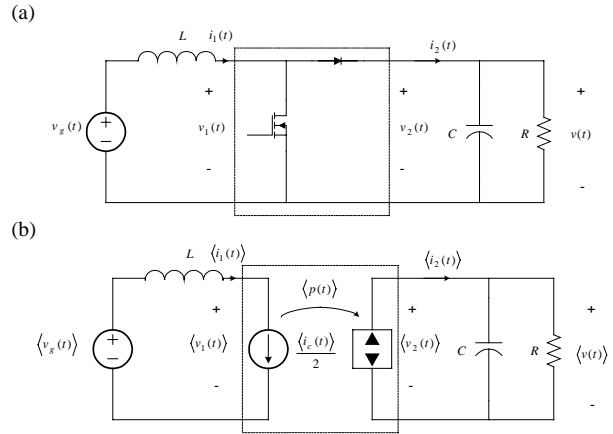


Fig. 3 (a) Boost converter example, with switch network identified, (b) averaged switch model

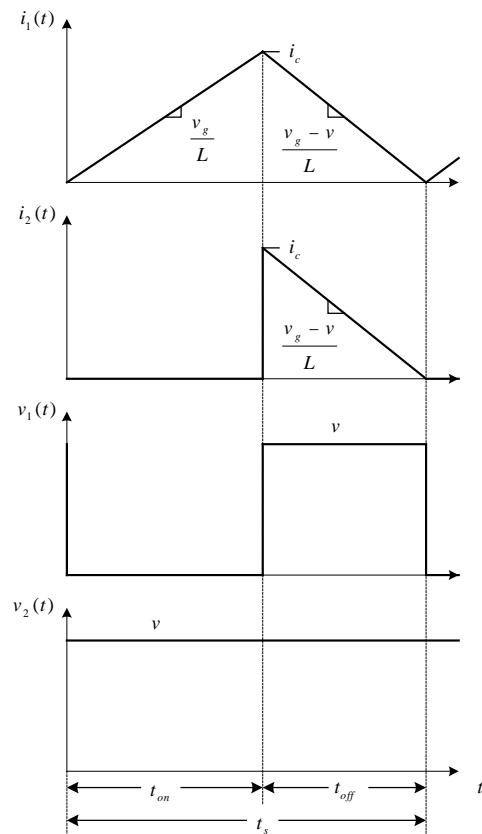


Fig. 4 Switch network current and voltage waveforms of BCM boost converter

control input. Therefore, the input port can be modeled as an independent current source, as shown in Fig. 3(b). The power consumed by the current source at the input port is transferred to the output port as shown by (5):

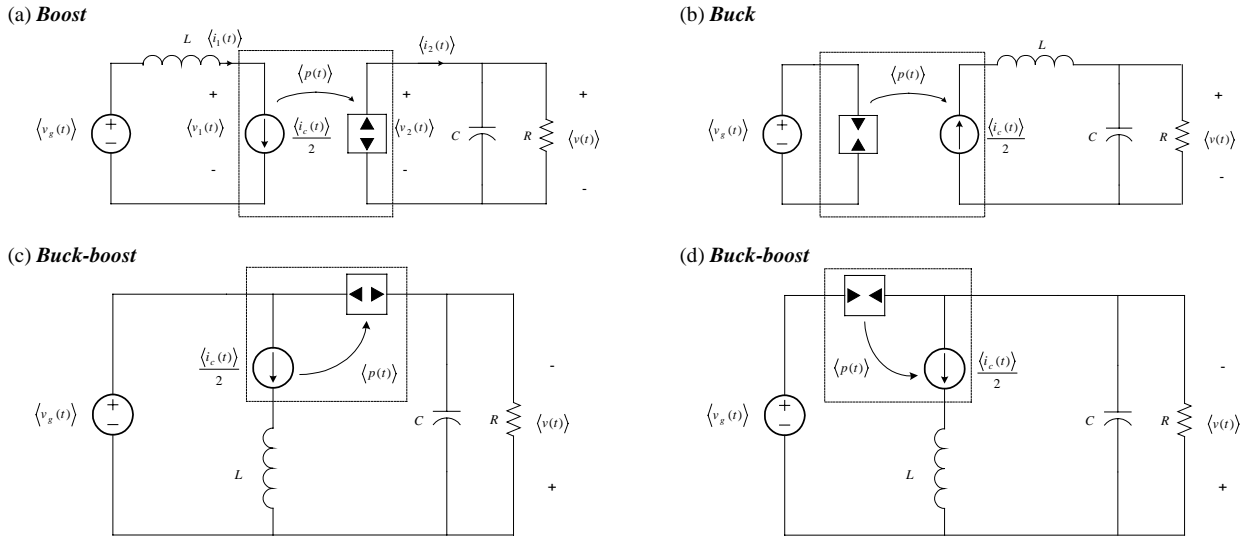


Fig. 5 Averaged large-signal equivalent circuits of basic converters operating in boundary conduction mode.

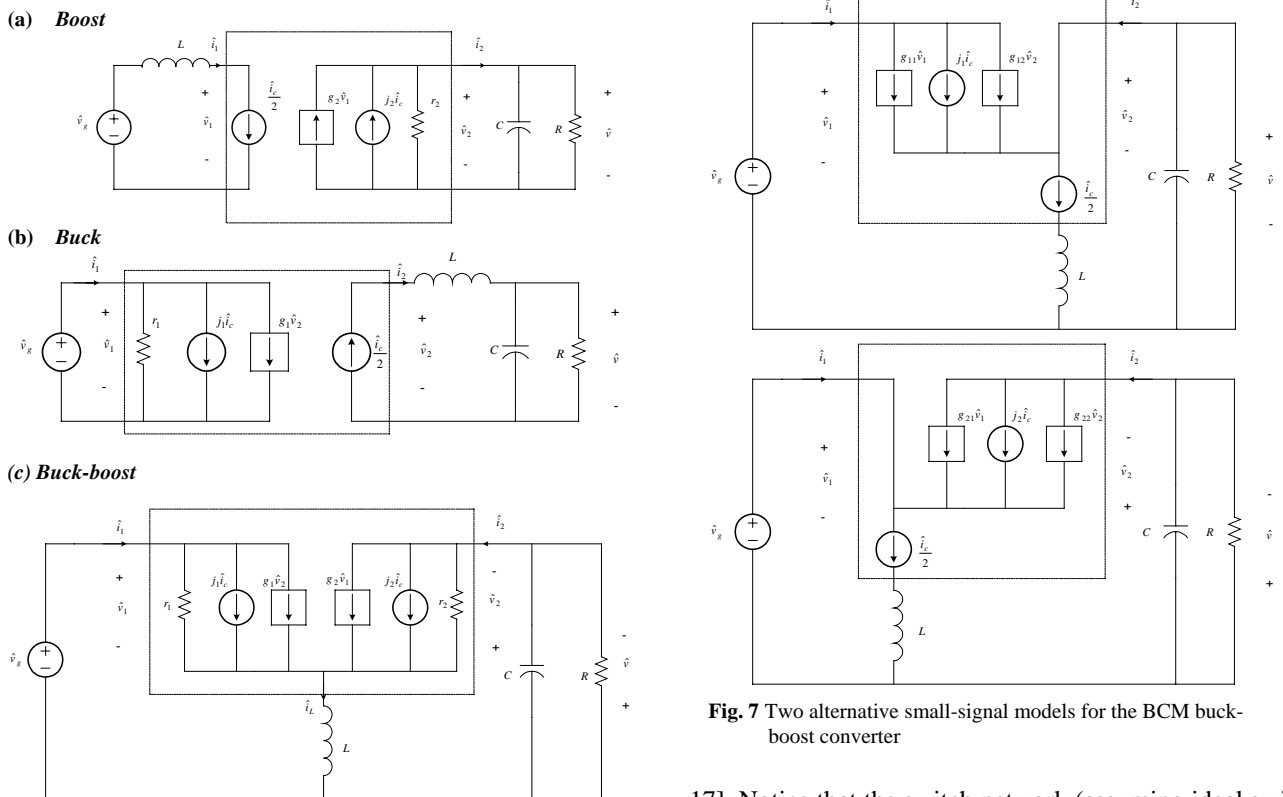


Fig. 6 Small-signal models of basic BCM converters

Fig. 7 Two alternative small-signal models for the BCM buck-boost converter

$$\langle v_1(t) \rangle \langle i_1(t) \rangle = \langle v_2(t) \rangle \langle i_2(t) \rangle = \langle p(t) \rangle \quad (5)$$

Therefore, the output port behaves as a dependent power source. The use and properties of dependent power source and power sink circuit elements have been described in [1,15-

17]. Notice that the switch network (assuming ideal switches) only transfers power, and exhibits loss-free characteristic.

By properly defining the switch network, the averaged switch models of BCM boost, buck, buck-boost converters, as well as BCM SEPIC and Cuk converters can be derived in the same manner, and the results are shown in Fig. 5. Again, a current source and a power source or a power sink appear in the equivalent circuit models.

TABLE I SMALL-SIGNAL BCM SWITCH MODEL PARAMETERS

Converter	j_1	r_1	g_1	j_2	r_2	g_2
Buck	$\frac{M}{2}$	$-\frac{R}{M^2}$	$\frac{M}{R}$	$\frac{1}{2}$	∞	0
Boost	$\frac{1}{2}$	∞	0	$\frac{1}{2M}$	R	$\frac{M}{R}$
Buck-Boost	$\frac{M}{2(M+1)}$	$-\frac{(M+1)R}{M^2}$	$\frac{M}{(M+1)R}$	$\frac{1}{2(M+1)}$	$\frac{(M+1)R}{M}$	$\frac{M^2}{(M+1)R}$

B. Small-signal model

The models of Fig. 3(b) and Fig. 5 are large-signal, nonlinear averaged models. Small-signal models are constructed by linearization of the large-signal averaged expressions. For the resulting linear, two-port network, we have:

$$\hat{i}_1 = j_1 \hat{i}_c + g_1 \hat{v}_2 + \frac{1}{r_1} \hat{v}_1 \quad (6)$$

$$\hat{i}_2 = j_2 \hat{i}_c + g_2 \hat{v}_1 - \frac{1}{r_2} \hat{v}_2 \quad (7)$$

The complete small-signal circuit model is obtained by replacing the switch network with the two-port network described by (6) and (7), as shown in Fig. 6. The expressions for the model parameters are summarized in Table I. M in the table represents the voltage conversion ratio.

In the equivalent circuits for the boost and the buck converter, the inductor is in series with the input current source, so the inductor dynamics (at low frequencies) are insignificant. In fact, the system transfer functions have only one pole due to the capacitor dynamics, while the inductor only has an effect on the zero.

In the BCM buck-boost converter, the following expression is always true:

$$\hat{i}_L = \hat{i}_1 + \hat{i}_2 = \frac{\hat{i}_c}{2} \quad (8)$$

As a result, the small-signal equivalent circuit for the BCM buck-boost converter can be simplified to one of the two alternatives illustrated in Fig. 7. The same conclusions about

TABLE II SALIENT FEATURES OF BCM CONVERTERS SMALL-SIGNAL TRANSFER FUNCTIONS

Converter	G_{vg0}	G_{vi0}	f_p	f_z
Buck	0	$\frac{R}{2}$	$\frac{1}{2\pi RC}$	∞
Boost	$\frac{M}{2}$	$\frac{R}{2M}$	$\frac{1}{\pi RC}$	$\frac{R}{2\pi L} \frac{1}{M^2}$
Buck-Boost	$\frac{M^2}{2M+1}$	$\frac{R}{2(2M+1)}$	$\frac{1}{2\pi RC} \frac{2M+1}{M+1}$	$\frac{R}{2\pi L} \frac{1}{M(M+1)}$

the inductor dynamics can be drawn for the BCM buck-boost converter as for the BCM buck and boost converters.

Transfer functions of interest can be found by solving the small-signal equivalent circuits. For the BCM buck, boost and buck-boost converters, the results for the control-to-output and the line-to-output transfer functions are given by (9) and (10), respectively. The salient features of transfer functions are summarized in Table II.

$$G_{vi} = G_{vi0} \left(1 - \frac{s}{\omega_z}\right) \left(1 + \frac{s}{\omega_p}\right) \quad (9)$$

$$G_{vg} = G_{vg0} \left(1 + \frac{s}{\omega_p}\right) \quad (10)$$

C. Comparison of BCM and constant-frequency current programmed control

The small-signal and large-signal equivalent circuits of BCM converters resemble the approximate low-frequency models of CCM current programmed control (CPM) [1,11,18,19]. The simple models of CCM CPM control have the same poles and zeros, and the same line-to-output dc gain as BCM control, except that the control-to-output dc gain is doubled. The simple models for CCM CPM are accurate when the converter is working in deep continuous conduction mode and without any stabilizing (“artificial”) ramp added to help the stability, so that the averaged inductor current is approximately equal to the control input. For BCM control, without any approximation, the average inductor current is controlled directly by the control input. As a result, the BCM exhibits the same properties as the simple model for CCM CPM. Because of the smaller inductance in BCM, the RHP (right-half plane) zero that appears in the control to output transfer function in the boost and buck-boost converters will be at higher frequency than for CCM CPM.

In a more accurate model of CCM CPM control, the additional high frequency pole can affect the bandwidth and the phase margin in a closed-loop system. This is not the case in BCM converters. A distinct feature of the BCM buck converter is that the line-to-output transfer function is zero. The disturbance of the input voltage has no effect (at low frequencies) on the output voltage.

CPM converters have the period-doubling instability problem when the duty ratio is greater than one half. An

artificial ramp is usually added to avoid the instability. In BCM, the inductor current drops to zero at the end of each switching cycle, so that the period-doubling instability cannot occur and no artificial ramp is needed.

IV. BOUNDARY CONDUCTION MODE WITH INPUT VOLTAGE FEEDFORWARD

BCM boost converter is frequently used in low-harmonic power factor correction (PFC) applications [2]. It has been found in [3] and [4] that BCM flyback and SEPIC also have acceptable performance as low-harmonic rectifiers. Similar to the discontinuous conduction mode (DCM), the input port of converters operating in BCM has inherent resistive or near-resistive characteristic.

As shown in Fig. 2, the BCM control input, i.e. the peak transistor current, is obtained by multiplication of a signal proportional to the input voltage and a control signal obtained at the output of a voltage-loop error amplifier. A low-bandwidth voltage regulator is used in single-phase PFC applications. Therefore, the control signal from the voltage-loop error amplifier is essentially constant during one half of the ac line cycle. As a result, the peak transistor current in the BCM converter with input voltage feedforward follows the shape of the input voltage waveform (which is a full-wave rectified sinusoidal waveform in PFC applications). Consequently, the averaged input current of the BCM boost converter follows the same waveshape.

With input voltage feedforward, the peak transistor current control $i_c(t)$ can be written as :

$$\langle i_c(t) \rangle = K \langle v_g(t) \rangle \langle v_c(t) \rangle \quad (11)$$

where $v_c(t)$ is the control input signal. Equation (1) can be rewritten as:

$$\langle i_1(t) \rangle = \frac{K}{2} \langle v_g(t) \rangle \langle v_c(t) \rangle \quad (12)$$

To derive an averaged switch model, we can assume that the converter is working in steady state, so that the average voltage on the inductor is zero,

$$\langle v_g(t) \rangle = \langle v_1(t) \rangle \quad (13)$$

The average input current becomes

$$\langle i_1(t) \rangle = \frac{K}{2} \langle v_1(t) \rangle \langle v_c(t) \rangle = \frac{\langle v_1(t) \rangle}{R_e} \quad (14)$$

where, $R_e = 2/(K \langle v_c(t) \rangle)$. According to (14), the input port of the BCM boost with input voltage feedforward behaves like a resistor. The independent current source in the large-signal model can be replaced by an emulated resistor R_e . This result can be extended to the buck-boost, SEPIC and Cuk converters. The averaged switch models for the BCM boost, buck-boost and SEPIC converters with input voltage feedforward are shown in Fig. 8.

The input current of the BCM buck-boost or SEPIC based rectifier can be easily derived from the large-signal model:

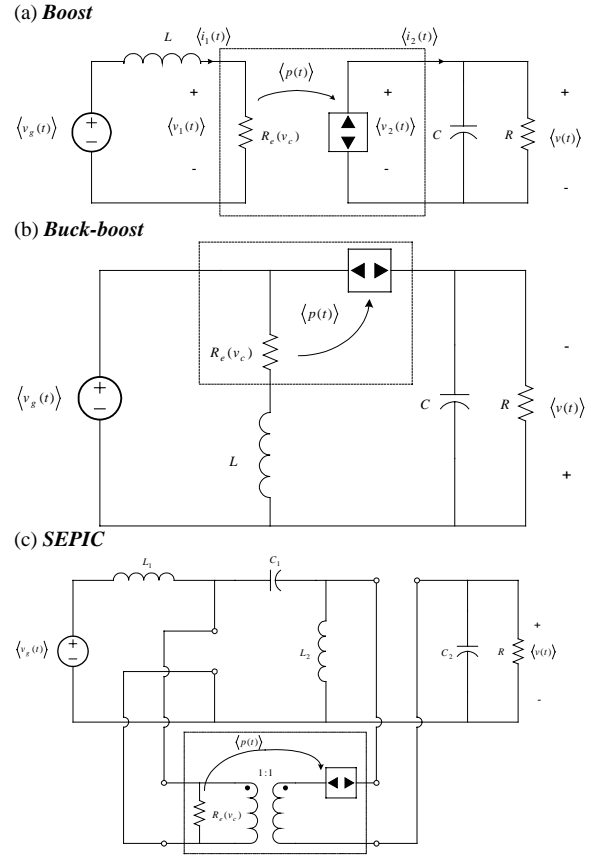


Fig. 8 Averaged switch model of basic BCM converters with input voltage feedforward.

$$\langle i_1(t) \rangle = \left\langle \frac{v_g(t)}{R_e} \right\rangle + \left\langle \frac{v_g^2(t)}{(v_g(t) + v)R_e} \right\rangle \quad (15)$$

The second term in (15) will introduce distortion into the input current as shown in [3] and [4]. Nevertheless, relatively low input current harmonics can be still achieved.

V. SIMULATION AND EXPERIMENTAL RESULTS

A feature of averaged switch models is that computer simulation can be easily performed using circuit-oriented simulation tools (such as PSpice). The large-signal averaged circuit model can be used in dc, transient and small-signal ac simulations. As an example, the control-to-output and line-to-output responses of the BCM boost converter are shown in Fig. 9, as obtained by PSpice ac simulation. The simulation results agree with the analytical results of Section III.

An experimental BCM boost prototype was built to measure the control-to-input transfer function. The measured magnitude and phase responses are shown in Fig. 10, and compared with the simulation results. Very good agreement between the model predictions and the measurements is obtained in a wide range of frequencies.

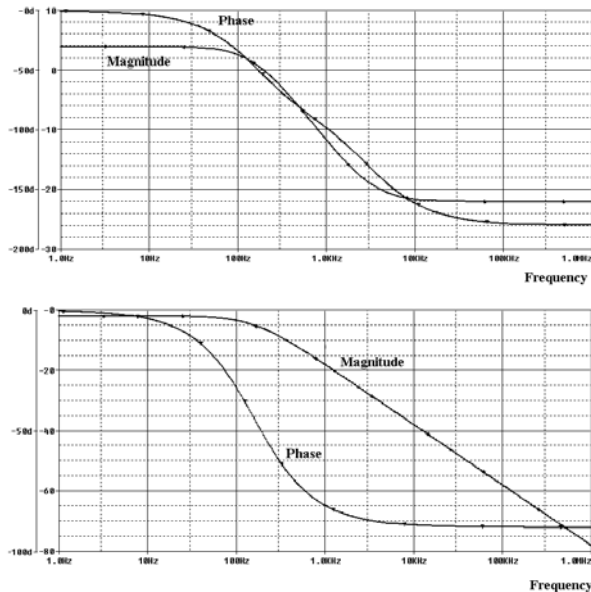
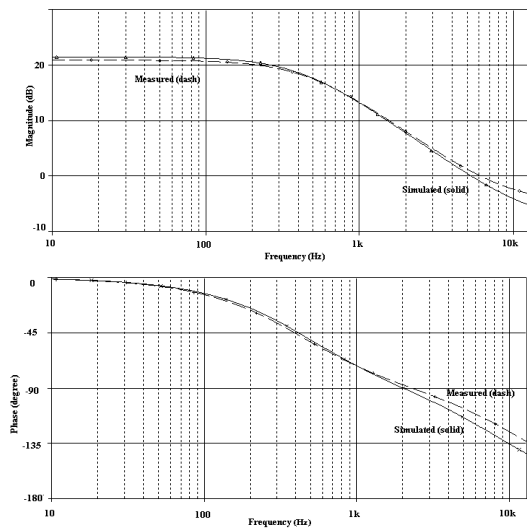


Fig. 9 Control-to-output transfer function (top) and line-to-output transfer function of BCM boost without input voltage feedforward.



$V_g=20V$, $V=34V$, $L=250\mu H$, $R=70V$, $f_s=20KHz$, $f_p=300Hz$,
 $f_c=16KHz$

Fig. 10 Measurement (dash) and simulation (solid) results comparison for BCM boost converter.

VI. CONCLUSIONS

In this paper, the averaged switch approach is extended to the modeling of dc-to-dc converters operating in boundary conduction mode (BCM), with or without input voltage feedforward. Large-signal and small-signal averaged-switch models lead to simple circuit models of BCM converters suitable for analysis or computer simulation. It is shown that BCM converters exhibit simpler dynamics compared to CCM current programmed control (CPM). Several BCM converters with input voltage feedforward feature resistive or nearly

resistive input characteristic, which is well suited for realization of power factor correctors. PSpice simulations and experimental results are used to verify validity of BCM averaged switch models in predicting converter frequency responses.

REFERENCES

- [1] R. W. Erickson and D. Maksimovic, *Fundamentals of Power Electronics*, Second Edition, Kluwer Academic Publishers, 2000.
- [2] J. Lai and D. Chen, "Design Consideration for Power Factor Correction Boost Converter Operating at the Boundary of Continuous Conduction Mode and Discontinuous Conduction Mode," *IEEE Applied Power Electronics Conference*, 1993 Record, pp. 267-273.
- [3] C. Adragna, "Design Equations of High-Power-Factor Flyback Converters Based on the L6561," *Application Note AN1059*, ST.
- [4] J. Chen and C. Chang, "Analysis and Design of SEPIC Converter in Boundary Conduction Mode for Universal-Line Power Factor Correction Applications," *IEEE Power Electronics Specialists Conference*, 2001 Record.
- [5] V. Vorperian, "Quasi-Square Wave Converters: Topologies and Analysis," *IEEE Transactions on Power Electronics*, Vol. 3, No.2, April 1988, pp. 183-191.
- [6] G. W. Wester and R. D. Middlebrook, "Low-Frequency Characterization of Switched Dc-Dc Converters," *IEEE Transactions on Aerospace and Electronic Systems*, Vol. AES-9, pp. 376-385, May 1973.
- [7] R. D. Middlebrook and Slobodan Cuk, "A General Unified Approach to Modeling Switching-Converter Power Stages," *International Journal of Electronics*, Vol. 42, No. 6, pp. 521-550, June 1977.
- [8] P. T. Krein, J. Bentsman, R. M. Bass, and B. C. Lesieutre, "On the Use of Averaging for the Analysis of Power Electronic Systems," *IEEE Transactions on Power Electronics*, Vol. 5, No. 2, pp. 182-190, April 1990.
- [9] S. Freeland and R. D. Middlebrook, "A Unified Analysis of Converters with Resonant Switches," *IEEE Power Electronics Specialists Conference*, 1987 Record, pp. 20-30.
- [10] V. Vorperian, R. Tymerski, and F. C. Lee, "Equivalent Circuit Models for Resonant and PWM Switches," *IEEE Transactions on Power Electronics*, Vol. 4, No. 2, pp. 205-214, April 1989.
- [11] V. Vorperian, "Simplified Analysis of PWM Converters Using the Model of the PWM Switch: Part I and II," *IEEE Transactions on Aerospace and Electronic Systems*, Vol. AES-26, pp. 409-505, May 1990.
- [12] A. Witulski and R. Erickson, "Extension of State-Space Averaging to Resonant Switches – and Beyond," *IEEE Transactions on Power Electronics*, Vol. 5, No. 1, pp. 98-109, January 1990.
- [13] D. Maksimovic and S. Cuk, "A Unified Analysis of PWM Converters in Discontinuous Modes," *IEEE Transactions on Power Electronics*, Vol. 6, No. 3, pp. 476-490, July 1991.
- [14] R. W. Erickson, "Advances in Averaged Switch Modeling," *Fourth Brazilian Congress of Power Electronics (COBEP97)*, December 1997, invited paper.
- [15] S. Singer, "Realization of Loss-Free Resistor Elements," *IEEE Transactions on Circuits and Systems*, Vol. CAS-36, No. 12, January 1990.
- [16] S. Singer and R. W. Erickson, "Power-Source Element and Its Properties," *IEEE Proceedings – Circuits Devices and Systems*, Vol. 141, No. 3, pp. 220-226, June 1994.
- [17] S. Singer and R. W. Erickson, "Canonical Modeling of Power Processing Circuits Based on the POPI Concept," *IEEE Transactions on Power Electronics*, Vol. 7, No. 1, January 1992.
- [18] G. Verghese, C. Bruzos, and K. Mahabir, "Averaged and Sampled-Data Models for Current Mode Control: A Reexamination," *IEEE Power Electronics Specialists Conference*, 1989 Record, pp. 484-491.
- [19] R. D. Middlebrook, "Modeling Current Programmed Buck and Boost Regulators," *IEEE Transactions on Power Electronics*, Vol. 4, No. 1 January 1989, pp. 36-52.